

Microstructure and transformation behavior of $\text{Ni}_{54}\text{Mn}_{25}\text{Ga}_{15}\text{Al}_6$ high-temperature shape memory alloy

Yan XIN¹, Yan LI²

1. School of Energy, Power and Mechanical Engineering, North China Electric Power University, Beijing 102206, China;
2. School of Materials Science and Engineering, Beihang University, Beijing 100191, China

Received 11 December 2012; accepted 13 April 2013

Abstract: The microstructure, martensitic transformation behavior, mechanical properties and shape memory effect of $\text{Ni}_{54}\text{Mn}_{25}\text{Ga}_{15}\text{Al}_6$ high-temperature shape memory alloy were investigated. By comparing with the $\text{Ni}_{54}\text{Mn}_{25}\text{Ga}_{21}$ alloy, the effect of Al addition on the properties of Ni–Mn–Ga alloys was analyzed. The results show that the $\text{Ni}_{54}\text{Mn}_{25}\text{Ga}_{15}\text{Al}_6$ alloy has a single-phase tetragonal non-modulated martensite structure with lamellar twins. The martensitic transformation start temperature of this alloy is up to 190 °C, displaying the promising application as a high-temperature shape memory alloy. Al addition in Ni–Mn–Ga alloy can decrease the martensitic transformation temperatures due to the effect of size factor and improve the strength and plasticity. However, the shape memory effect is reduced remarkably with the Al addition.

Key words: shape memory alloy; Ni–Mn–Ga; Al addition; martensitic transformation

1 Introduction

In the last decade, Ni_2MnGa ferromagnetic shape memory alloys have been extensively explored as candidates for magnetic actuator materials due to their large magnetic-field-induced strains [1–4]. Meanwhile, these alloys also undergo a thermoelastic martensitic transformation under cooling. It has been demonstrated that the martensitic transformation temperature of the off-stoichiometric Ni_2MnGa alloys is very sensitive to the composition ranging from liquid helium temperature up to over 350 °C [5,6]. Accordingly, some Ni-rich Ni_2MnGa alloys were developed as promising high temperature shape memory alloys with well-defined shape memory effects [7–9], good superelasticity [10] and high thermo-cycling stability [11]. These excellent properties and relatively low cost made Ni–Mn–Ga alloys more promising than other high-temperature shape memory alloys, such as Ti–Ni–Hf, Cu–Al–Ni and Ti–Ni–Pd alloys.

It is known that the polycrystalline Ni–Mn–Ga alloys are extremely brittle although their single crystals exhibit very high mechanical strain of about 20% [7].

The rod sample prepared by LI et al [8] showed that grain refinement is an effective method to improve the mechanical and shape memory characteristics of $\text{Ni}_{54}\text{Mn}_{25}\text{Ga}_{21}$ alloys. The compressive strength and compressive strain of the button sample are 440 MPa and 10%, respectively, and the corresponding values of the rod sample are 970 MPa and 16%, respectively. On the other hand, many efforts have been made to improve the plasticity of Ni–Mn–Ga alloy by adding the fourth element, such as Fe, Ti, Co, Cu, Cr, Gd or rare elements [12–20]. The ductility has been improved by introducing sufficient amount of ductile γ phase in the Ni–Mn–Ga alloys with Fe, Co, Cu or Cr additions [12,14,16–18]. However, little information about the addition of Al into Ni–Mn–Ga alloys has been reported up to now. The purpose of this work is to investigate the microstructure, transformation behavior, mechanical properties and shape memory effect of $\text{Ni}_{54}\text{Mn}_{25}\text{Ga}_{15}\text{Al}_6$ alloy to show the effect of Al addition on the properties of Ni–Mn–Ga alloys.

2 Experimental

The polycrystalline button ingots with the nominal

composition of $\text{Ni}_{54}\text{Mn}_{25}\text{Ga}_{15}\text{Al}_6$ and $\text{Ni}_{54}\text{Mn}_{25}\text{Ga}_{21}$ alloy were prepared with high-purity Ni (99.9%), Mn (99.9%), Ga (99.99%) and Al (99.99%) by melting 4 times in an arc-melting furnace under argon atmosphere. $\text{Ni}_{54}\text{Mn}_{25}\text{Ga}_{21}$ alloy was prepared for comparison. Some button ingots of these alloys were re-melted into rods of approximately 6.8 mm in diameter using a cylindrical copper mold which was set at the bottom of the furnace. The rod ingots sealed in vacuum quartz ampoules were annealed at 1000 °C for 24 h followed by water quenching. Some slices with 1 mm thickness were cut down from the as-quenched rod alloys by an electro-discharge machine for microstructure observation and phase structure analysis. The samples for phase transformation measurement were cut down from the slices by a slow-speed diamond saw.

The microstructures were observed by optical microscopy (OM) and transmission electron microscopy (TEM, Hitachi H-800 operating at 200 kV). Samples for OM observation were mechanically polished and chemically etched in a solution of 4 g CuSO_4 + 20 mL hydrochloric acid (HCl) + 20 mL H_2O . The phase structure was identified at room temperature by X-ray diffraction (XRD, Rigaku D/Max 2200PC diffractometer with Cu K_α radiation). The phase transformation temperatures of the alloy were measured by differential scanning calorimetry (DSC, Perkin-Elmer DSC-7) with a cooling/heating rate of 10 °C/min.

From the middle part of the rod alloy, some samples with dimensions of $d3 \text{ mm} \times 5 \text{ mm}$ were also cut for mechanical property testing. Compressive stress–strain curves were tested by a MTS-800 master material tester at room temperature. The shape memory effect of the samples was measured after unloading. The height of the samples was measured before loading (h_0), after loading (h_1) and after heating to 400 °C for 15 min (h_2) by a micrometer with an accuracy of 0.01 mm. The shape memory strains were obtained as: $(h_2 - h_1)/h_0 \times 100\%$. The recovery ratio (R) was calculated as: $(h_2 - h_1)/(h_0 - h_1) \times 100\%$.

3 Results and discussion

3.1 Microstructure

The powder XRD patterns of the as-quenched $\text{Ni}_{54}\text{Mn}_{25}\text{Ga}_{15}\text{Al}_6$ and $\text{Ni}_{54}\text{Mn}_{25}\text{Ga}_{21}$ alloys are shown in Fig. 1. The reflection peaks in the XRD pattern of $\text{Ni}_{54}\text{Mn}_{25}\text{Ga}_{15}\text{Al}_6$ alloy can be indexed with the unique tetragonal non-modulated martensite phase, identical to that of the single-phase $\text{Ni}_{54}\text{Mn}_{25}\text{Ga}_{21}$ alloy. Therefore, substituting Al for Ga in Ni–Mn–Ga alloy doesn't introduce any new phase, which is different from the Ni–Mn–Ga alloys with Fe, Co, Cu, Cr, Gd additions [12,14,16–19]. By calculating from the XRD results, the

crystal lattice parameters of martensite phase in $\text{Ni}_{54}\text{Mn}_{25}\text{Ga}_{15}\text{Al}_6$ alloy are $a=b=0.7664 \text{ nm}$, $c=0.6631 \text{ nm}$, $c/a=0.8652$ and the corresponding unit-cell volume is 0.3895 nm^3 . In comparison, the crystal lattice parameters of martensitic phase in $\text{Ni}_{54}\text{Mn}_{25}\text{Ga}_{21}$ alloy are $a=b=0.7656 \text{ nm}$, $c=0.6633 \text{ nm}$, $c/a=0.8664$ and the corresponding unit-cell volume is 0.3888 nm^3 . It can be seen that the crystal lattice parameter c almost has no change but the a parameter increases with substituting Al for Ga in the $\text{Ni}_{54}\text{Mn}_{25}\text{Ga}_{21}$ alloy, which leads to a reduction in tetragonality (c/a). Simultaneously, substituting Al for Ga in Ni–Mn–Ga alloy expands the unit-cell volume.

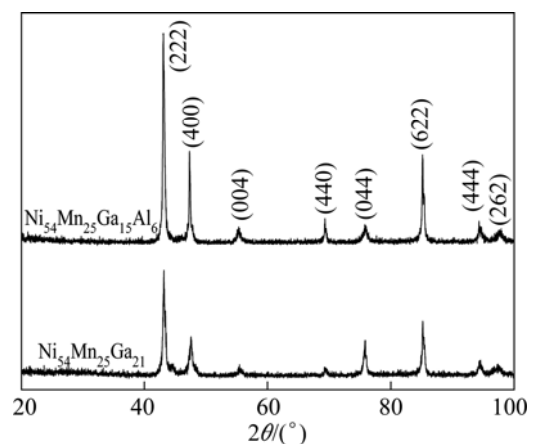


Fig. 1 Powder XRD patterns of $\text{Ni}_{54}\text{Mn}_{25}\text{Ga}_{15}\text{Al}_6$ and $\text{Ni}_{54}\text{Mn}_{25}\text{Ga}_{21}$ alloys

The XRD measurement result can also be confirmed by microstructure observation. Figure 2 shows the optical micrograph, TEM images and selected area electron diffraction (SAED) pattern of the as-quenched $\text{Ni}_{54}\text{Mn}_{25}\text{Ga}_{15}\text{Al}_6$ alloy. It can be obviously observed in Fig. 2(a) that this alloy has a single martensite phase structure with lamellar twins. The TEM bright-field image in Fig. 2(b) shows that the martensite variants are twinned and well self-accommodated. Figure 2(c) is the enlargement of the framed area B in Fig. 2(b), which shows that each variant has high-density inner microtwins. The corresponding SAED pattern of the circle area A in Fig. 2(b) is shown in Fig. 2(d). Twin-related double sets of reflections are observed in this SAED pattern, which can be identified as a tetragonal non-modulated martensite structure, as shown in Fig. 2(d).

3.2 Martensitic transformation behavior

Figure 3 shows the DSC curves of $\text{Ni}_{54}\text{Mn}_{25}\text{Ga}_{15}\text{Al}_6$ alloy. The endothermic peak on the heating curve is associated with the reverse martensitic transformation from tetragonal martensite to cubic austenite, where the reverse martensitic transformation start temperature (A_s),

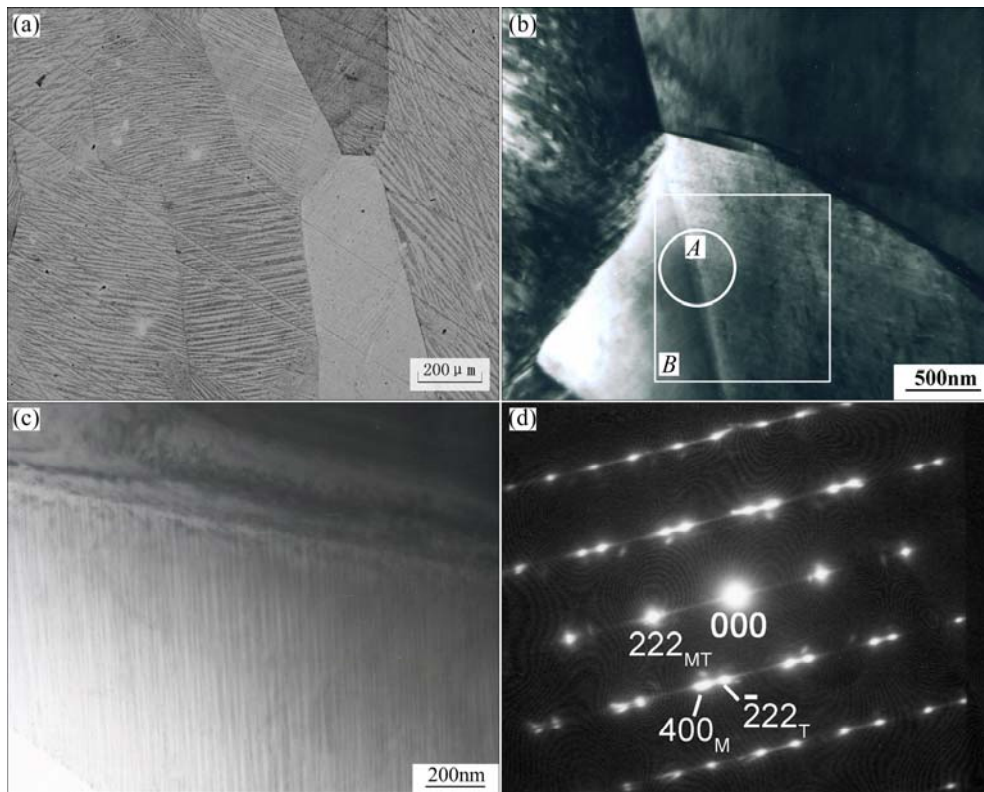


Fig. 2 Microstructures and SAED pattern of $\text{Ni}_{54}\text{Mn}_{25}\text{Ga}_{15}\text{Al}_6$ alloy: (a) Optical micrograph; (b) TEM bright-field image of martensite; (c) Enlargement of framed area *B* in (b); (d) SAED pattern taken from circled area *A* in (b)

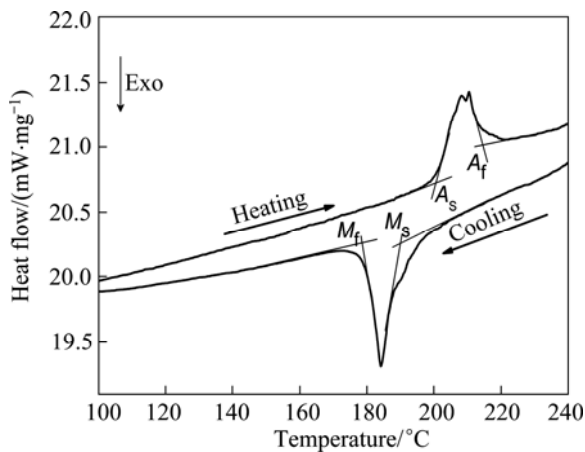


Fig. 3 DSC curves of as-quenched $\text{Ni}_{54}\text{Mn}_{25}\text{Ga}_{15}\text{Al}_6$ alloy

peak temperature (A_p) and finish temperature (A_f) are 202, 210 and 214 °C, respectively. The exothermic peak occurring on the cooling curve indicates the forward martensitic transformation with the start temperature (M_s), peak temperature (M_p) and finish temperature (M_f) of 190, 184 and 179 °C, respectively. The corresponding temperatures of A_s and M_s for $\text{Ni}_{54}\text{Mn}_{25}\text{Ga}_{21}$ alloy are 273 and 260 °C, respectively. Therefore, Al addition in Ni–Mn–Ga alloy can reduce the martensitic transformation temperatures. The transformation temperature (M_s) of the $\text{Ni}_{54}\text{Mn}_{25}\text{Ga}_{15}\text{Al}_6$ alloy is still as high as about 190 °C, much higher than room

temperature, which means this alloy can be used as a high-temperature shape memory alloy. It is acknowledged that the electron concentration of martensite and the size factor (the unit-cell volume and the tetragonality c/a) can affect the transformation temperatures of the Ni–Mn–Ga based alloys [18,21]. Since Al and Ga belong to the same family with the same number of outer electrons, no electron concentration changes during substituting Al for Ga in Ni–Mn–Ga alloy. Thus, the decrease of the transformation temperatures by substituting Al for Ga is attributed to the size factor changes, that is, the reduction of tetragonality (c/a) and expansion of the unit-cell volume, as obtained from the XRD results in section 3.1. A smaller tetragonality (c/a) of martensite indicates less lattice deformation and less energy variation during the martensitic transformation, which leads to lower martensitic transformation temperatures. These results are consistent with the previous works [15,16,18,21].

3.3 Mechanical and shape memory properties

The compressive stress–strain curves of the $\text{Ni}_{54}\text{Mn}_{25}\text{Ga}_{21}$ and $\text{Ni}_{54}\text{Mn}_{25}\text{Ga}_{15}\text{Al}_6$ alloys are shown in Fig. 4, in which Curve a and Curve b correspond to $\text{Ni}_{54}\text{Mn}_{25}\text{Ga}_{21}$ and $\text{Ni}_{54}\text{Mn}_{25}\text{Ga}_{15}\text{Al}_6$ alloys, respectively. These two curves were obtained by compressing the sample until it cracked. The compressive fracture

strength and strain of the $\text{Ni}_{54}\text{Mn}_{25}\text{Ga}_{21}$ alloy are 873 MPa and 14.3%, respectively, and the corresponding values of the $\text{Ni}_{54}\text{Mn}_{25}\text{Ga}_{15}\text{Al}_6$ alloy are 1027 MPa and 15.8%, respectively. Therefore, Al substitution for Ga can improve the fracture strength and plasticity of Ni–Mn–Ga alloy due to the solid solution of Al atoms, which is similar to the Ti–Ni–Al alloy [22].

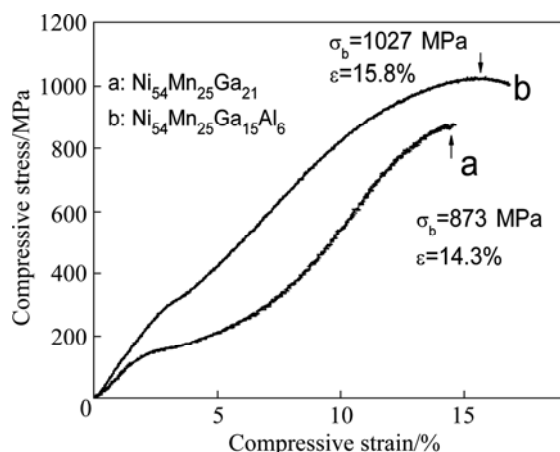


Fig. 4 Compressive stress–strain curves of $\text{Ni}_{54}\text{Mn}_{25}\text{Ga}_{21}$ (a) and $\text{Ni}_{54}\text{Mn}_{25}\text{Ga}_{15}\text{Al}_6$ (b) alloys

In order to investigate the shape memory effect, the $\text{Ni}_{54}\text{Mn}_{25}\text{Ga}_{15}\text{Al}_6$ and $\text{Ni}_{54}\text{Mn}_{25}\text{Ga}_{21}$ alloys were compressed at room temperature to different total strains (4%–10%). The compressive stress–strain curve at total strain of 8% for $\text{Ni}_{54}\text{Mn}_{25}\text{Ga}_{15}\text{Al}_6$ alloy is shown in Fig. 5 and the arrowed line represents the shape memory strain after heating to 400 °C. The residual strain after unloading is 3.6%. The shape memory strain is 1% and the recovery ratio is 22%. The shape memory strain and recovery ratio of the $\text{Ni}_{54}\text{Mn}_{25}\text{Ga}_{15}\text{Al}_6$ and $\text{Ni}_{54}\text{Mn}_{25}\text{Ga}_{21}$ alloy at different total strains are shown in Fig. 6. It can be seen that the maximum shape memory strain of $\text{Ni}_{54}\text{Mn}_{25}\text{Ga}_{15}\text{Al}_6$ alloy is 1% at the total strain of 6% and 8% with the recovery ratio of 36% and 22%, respectively.

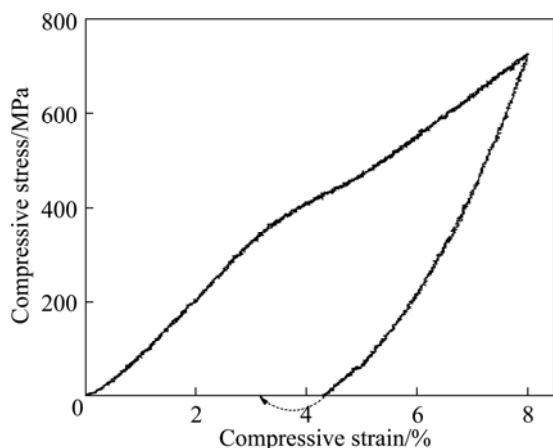


Fig. 5 Compressive stress–strain curve of $\text{Ni}_{54}\text{Mn}_{25}\text{Ga}_{15}\text{Al}_6$ alloy with 8% total strain

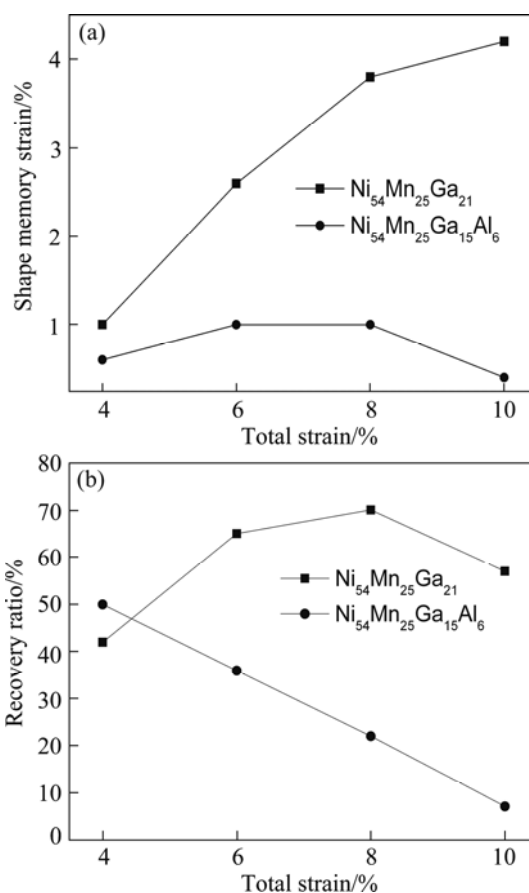


Fig. 6 Shape memory strain (a) and recovery ratio (b) of $\text{Ni}_{54}\text{Mn}_{25}\text{Ga}_{15}\text{Al}_6$ and $\text{Ni}_{54}\text{Mn}_{25}\text{Ga}_{21}$ alloys

While the maximum shape memory strain of $\text{Ni}_{54}\text{Mn}_{25}\text{Ga}_{21}$ alloy is 4.2% at the total strain of 10% with the recovery ratio of 57%. Consequently, the shape memory effect of $\text{Ni}_{54}\text{Mn}_{25}\text{Ga}_{15}\text{Al}_6$ alloy is worse than that of $\text{Ni}_{54}\text{Mn}_{25}\text{Ga}_{21}$ alloy. Similar to adding Cu and Cr [16,18], the shape memory effect is reduced remarkably with the Al addition.

4 Conclusions

1) The $\text{Ni}_{54}\text{Mn}_{25}\text{Ga}_{15}\text{Al}_6$ alloy has a single-phase tetragonal non-modulated martensite structure and the martensite variants are twinned and well self-accommodated.

2) The martensitic transformation start temperature of $\text{Ni}_{54}\text{Mn}_{25}\text{Ga}_{15}\text{Al}_6$ is up to 190 °C, displaying the promising application as a high-temperature shape memory alloy. Al addition in Ni–Mn–Ga alloy can reduce the martensitic transformation temperatures, which is attributed to the size factor changes, that is, the reduction of tetragonality (c/a) and expansion of the unit-cell volume.

3) Al substitution for Ga can improve the mechanical properties of the Ni–Mn–Ga alloy. The

compressive fracture strength and strain of the $\text{Ni}_{54}\text{Mn}_{25}\text{Ga}_{15}\text{Al}_6$ alloy are 1027 MPa and 15.8%, respectively. However, the shape memory effect is reduced remarkably with Al addition. The maximum shape memory strain of $\text{Ni}_{54}\text{Mn}_{25}\text{Ga}_{15}\text{Al}_6$ alloy is 1% at the total strain of 6% and 8% with the recovery ratio of 36% and 22%, respectively.

References

- [1] ULLAKKO K, HUANG J K, KANTNER C, O'HANDLEY R C, KOKORIN V V. Large magnetic-field-induced strains in Ni_2MnGa single crystals [J]. Applied Physics Letters, 1996, 69(13): 1966–1968.
- [2] MURRAY S J, MARIONI M, ALLEN S M, O'HANDLEY R C, LOGRASSO T A. 6% magnetic-field-induced strain by twin-boundary motion in ferromagnetic Ni–Mn–Ga [J]. Applied Physics Letters, 2000, 77(6): 886–888.
- [3] SOZINOV A, LIKHACHEV A, LANSKA N, ULLAKKO K. Giant magnetic-field-induced strain in NiMnGa seven-layered martensitic phase [J]. Applied Physics Letters, 2002, 80(10): 1746–1748.
- [4] CHMIELUS M, ZHANG X X, WITHERSPOON C, DUNAND D C, MULLNER P. Giant magnetic-field-induced strains in polycrystalline Ni–Mn–Ga foams [J]. Nature Materials, 2009, 8(11): 863–866.
- [5] CHERNENKO V A, CESARI E, KOKORIN V V, VITENKO I N. The development of new ferromagnetic shape memory alloys in Ni–Mn–Ga system [J]. Scripta Metallurgica et Materialia, 1995, 33(8): 1239–1244.
- [6] JIANG Cheng-bao, FENG Gen, GONG Sheng-kai, XU Hui-bin. Effect of Ni excess on phase transformation temperatures of NiMnGa alloys [J]. Materials Science and Engineering A, 2003, 342(1–2): 231–235.
- [7] XU Hui-bin, MA Yun-qing, JIANG Cheng-bao. A high-temperature shape-memory alloy $\text{Ni}_{54}\text{Mn}_{25}\text{Ga}_{21}$ [J]. Applied Physics Letters, 2003, 82(19): 3206–3208.
- [8] LI Yan, XIN Yan, JIANG Cheng-bao, XU Hui-bin. Shape memory effect of grain refined $\text{Ni}_{54}\text{Mn}_{25}\text{Ga}_{21}$ alloy with high transformation temperature [J]. Scripta Materialia, 2004, 51 (9): 849–852.
- [9] XIN Yan, LI Yan, CHAI Liang, XU Hui-bin. Shape memory characteristics of dual-phase Ni–Mn–Ga based high temperature shape memory alloys [J]. Scripta Materialia, 2007, 57(7): 599–601.
- [10] CHERNENKO V A, L'VOV V, PONS J, CESARI E. Superelasticity in high-temperature Ni–Mn–Ga alloys [J]. Journal of Applied Physics, 2003, 93(5): 2394–2399.
- [11] MA Yun-qing, JIANG Cheng-bao, FENG Gen, XU Hui-bin. Thermal stability of the $\text{Ni}_{54}\text{Mn}_{25}\text{Ga}_{21}$ Heusler alloy with high temperature transformation [J]. Scripta Materialia, 2003, 48(4): 365–369.
- [12] MA Yun-qing, XU Li-hong, LI Yan, JIANG Cheng-bao, XU Hui-bin, LEE Y K. Martensitic transformation, ductility, and shape-memory effect of polycrystalline $\text{Ni}_{56}\text{Mn}_{25-x}\text{Fe}_x\text{Ga}_{19}$ alloys [J]. Zeitschrift Fur Metallkunde, 2005, 96(8): 843–846.
- [13] DONG G F, CAI W, GAO Z Y, SUI J H. Effect of isothermal ageing on microstructure, martensitic transformation and mechanical properties of $\text{Ni}_{53}\text{Mn}_{23.5}\text{Ga}_{18.5}\text{Ti}_5$ ferromagnetic shape memory alloy [J]. Scripta Materialia, 2008, 58(8): 647–650.
- [14] MA Yun-qing, YANG Shui-yuan, LIU Yong, LIU Xing-jun. The ductility and shape-memory properties of Ni–Mn–Co–Ga high-temperature shape-memory alloys [J]. Acta Materialia, 2009, 57(11): 3232–3241.
- [15] SÁNCHEZ-ALARCO V, PÉREZ-LANDEZÁBAL J I, RECARTE V, GÓMEZ-POLO C, RODRÍGUEZ-VELAMAZÁN J A. Correlation between composition and phase transformation temperatures in Ni–Mn–Ga–Co ferromagnetic shape memory alloys [J]. Acta Materialia, 2008, 56(19): 5370–5376.
- [16] MA Yun-qing, YANG Shui-yuan, JIN Wan-jun, LIU Xing-jun. $\text{Ni}_{56}\text{Mn}_{25-x}\text{Cu}_x\text{Ga}_{19}$ ($x=0, 1, 2, 4, 8$) high-temperature shape-memory alloys [J]. Journal of Alloys and Compounds, 2009, 471(1–2): 570–574.
- [17] LI Ying-ying, WANG Jing-min, JIANG Cheng-bao. Study of Ni–Mn–Ga–Cu as single-phase wide-hysteresis shape memory alloys [J]. Materials Science and Engineering A, 2011, 528(22–23): 6907–6911.
- [18] MA Yun-qing, LAI San-li, YANG Shui-yuan, LUO Yu, WANG Cui-ping, LIU Xing-jun. $\text{Ni}_{56}\text{Mn}_{25-x}\text{Cr}_x\text{Ga}_{19}$ ($x=0, 2, 4, 6$) high temperature shape memory alloys [J]. Transactions of Nonferrous Metals Society of China, 2011, 21(1): 96–101.
- [19] GAO L, CAI W, LIU A L, ZHAO L C. Martensitic transformation and mechanical properties of polycrystalline $\text{Ni}_{50}\text{Mn}_{29}\text{Ga}_{21-x}\text{Gd}_x$ ferromagnetic shape memory alloys [J]. Journal of Alloys and Compounds, 2006, 425(1–2): 314–317.
- [20] TSUCHIYA K, TSUTSUMI A, OHTSUKA H, UMEMOTO M. Modification of Ni–Mn–Ga ferromagnetic shape memory alloy by addition of rare earth elements [J]. Materials Science and Engineering A, 2004, 378(1–2): 370–376.
- [21] MA Yun-qing, JIANG Cheng-bao, LI Yan, XU Hui-bin, WANG Cui-ping, LIU Xing-jun. Study of $\text{Ni}_{50+x}\text{Mn}_{25}\text{Ga}_{25-x}$ ($x=2-11$) as high-temperature shape-memory alloys [J]. Acta Materialia, 2007, 55(5): 1533–1541.
- [22] HSIEH S F, WU S K. A study on a $\text{Ti}_{52}\text{Ni}_{47}\text{Al}_1$ shape memory alloy [J]. Journal of Materials Science, 1999, 34(7): 1659–1665.

$\text{Ni}_{54}\text{Mn}_{25}\text{Ga}_{15}\text{Al}_6$ 高温形状记忆合金的微观组织和相变行为

辛燕¹, 李岩²

1. 华北电力大学 能源动力与机械工程学院, 北京 102206; 2. 北京航空航天大学 材料与工程学院, 北京 100191

摘要: 研究 $\text{Ni}_{54}\text{Mn}_{25}\text{Ga}_{15}\text{Al}_6$ 高温形状记忆合金的微观组织、马氏体相变特性、力学性能和形状记忆效应。通过与 $\text{Ni}_{54}\text{Mn}_{25}\text{Ga}_{21}$ 合金对比, 分析添加第四组元 Al 对 Ni–Mn–Ga 合金性能的影响。结果表明: $\text{Ni}_{54}\text{Mn}_{25}\text{Ga}_{15}\text{Al}_6$ 合金为单一的四方结构非调制马氏体相并呈片状的马氏体孪晶板条形貌。该合金的马氏体相变开始温度超过 190 °C, 具有发展成为高温形状记忆合金的潜力。在 Ni–Mn–Ga 合金中添加 Al 会降低马氏体相变温度, 这主要归因于 Al 添加引入的晶格尺寸因素的改变。添加 Al 元素能有效提高合金的强度和塑性, 但降低合金的形状记忆性能。

关键词: 形状记忆合金; Ni–Mn–Ga; Al 添加; 马氏体相变

(Edited by Chao WANG)